LLNL-CONF-599056

Incorporating Afterburn Effects Into A Fast-Running Tool for Modeling Explosives in Tunnels

S. Neuscamman, G. Pezzola, S. Alves, L. Glenn, L. Glascoe

November 6, 2012

JANNAF 45th Combustion
Monterey, CA, United States
December 3, 2012 through December 7, 2012

Disclaimer

INCORPORATING AFTERBURN EFFECTS INTO A FAST-RUNNING TOOL FOR MODELING EXPLOSIVES IN TUNNELS

S. J. Neuscamman, G. L. F. Pezzola, S. W. Alves, L. A. Glenn, L. G. Glascoe
Lawrence Livermore National Laboratory
Livermore, CA

ABSTRACT

A fast-running, physics-based tool has been developed at Lawrence Livermore National Laboratory to provide rapid and accurate predictions of blast effects and personnel fatality within an enclosed underground facility. STUNTool provides pressure histories, damage estimates, and injury estimates in an expedient manner, has been validated to experimental data, and is advocated by customers in the Department of Homeland Security Science and Technology Directorate (DHS S&T), who funded this effort, and the U.S. Army Corps of Engineers, Engineering Research and Development Center (ERDC). This paper describes recent efforts to enhance the tool to include representations of the sub-detonative physics of explosive afterburn. A modified version of the Jones-Wilkins-Lee (JWL) equation of state, which accounts for longer-time combustion effects and is termed the "JWLa," was developed in the high-fidelity hydrocode ALE3D and shows good agreement to experimental data. Initial efforts to implement the modified equation of state in the tunnel tool are discussed with the goal of using the afterburn model to allow users to estimate the effect on tunnel conditions, including tunnel damage and breach likelihood, of the additional energy released via afterburning.

INTRODUCTION

Although high performance computational hydrodynamic and structural analysis tools such as CTH or ALE3D (McGlaun 1990, Nichols 2009) can be used to predict the response of structures to shock loads, these tools require significant computational resources, and it is often difficult to conduct a timely assessment when a large range of threats or structural configurations are of interest. Further, when specifically considering tunnel systems, direct high-fidelity simulation of explosive effects is challenging due to a combination of factors. First, the flow in tunnels is dominated by boundary layer effects, which require fine radial resolution to capture. Second, the high length to diameter ratio characteristic of tunnels results in an extensive tunnel domain relative to tunnel diameter when down-tunnel effects are needed. These factors together make direct three-dimensional simulation of flow in long tunnels prohibitively expensive. Even two-dimensional (2D) simulations of extensive tunnel lengths can become too expensive when considering a multiparametric study.

A fast-running tool with two components that can be used to estimate the effects of explosive blasts in tunnels has been developed. One component utilizes a simplified algorithm, the sphere and tunnel (STUN) code, which captures the essential physics of shock propagation in tunnels, yet runs in seconds to minutes on a single processor (Glenn 2001). The code solves the 1D fluid flow equations of mass, momentum and energy. The explosive energy release is modeled using the JWL equation of state, and several explosive types are included. The effects of wall drag are accounted for in the momentum equation using a friction factor, *f*, which is a function of the Reynolds number. For simulation of an in-tunnel blast, STUN couples several 1D representations of the tunnel and blast into a higher dimensional representation. Specifically, the code solves a spherical flow problem for the detonation that is coupled to 1D axial flow through the tunnel segments. By varying the cross section of the tunnel along its length, it is possible to

----

Distribution Statement A: Approved for public release; distribution is unlimited.

This work was performed under the auspices of the U.S. Department of Energy by Lawrence Livermore National Laboratory under contract DE-AC52-07NA27344.

LLNL-CONF-599056

account for the effect of tunnel segments with larger cross-section (stations or platforms) and restricted cross section (trains) on the blast wave. STUN can predict the effect of an arbitrary number of bends in the tunnel system and supports coupling to additional tunnel segments to simulate the effect of tunnel intersections on the shock wave. This capability allows users to rapidly determine the loading environments associated with a range of credible threat configurations, locations, and even changes in the tunnel system.

The second component of the tool is a statistical emulator for predicting and bounding the close-in structural response at varying threat sizes and standoff distance using previously executed high fidelity analysis. High-fidelity analyses are conducted for a hypothetical steel-rebar reinforced concrete tunnel, (Figure 1). Charge weight, standoff and tunnel thicknesses are varied, with simulation conformations determined via a statistical algorithm to minimize the number of expensive runs required to accurately predict the boundary between breach and no breach cases (Glascoe 2012). Structural damage is quantified using a combined index of shear dilation and density change in the concrete. Both metrics indicate the separation of aggregate and mortar necessary for the formation of rubble. Compressive damage is tracked well by material dilation. Large dilation strains emulate a real-world loading scenario where aggregate has been separated violently from the mortar. Based on split Hopkinson pressure bar tests and expert analysis, a threshold volumetric strain from dilation is chosen to represent damage. Another indication of concrete damage severe enough to cause breach is a decrease in density which can be similarly compared to dynamic Brazilian split cylinder tests. Density is tracked by the constitutive material model and its decrease can be attributed to tensile failure in the form of cracking and spall. Once damage is evaluated and breach characterized, the results are compiled into breach curves that allow the user to quickly determine if damage to the tunnel is severe enough that a breach in the wall is likely for a range of threat conditions. Further description of the structural and statistical analyses employed to construct the breach curves can be found in Glascoe et al., 2012 and Lennox and Glascoe, 2011.

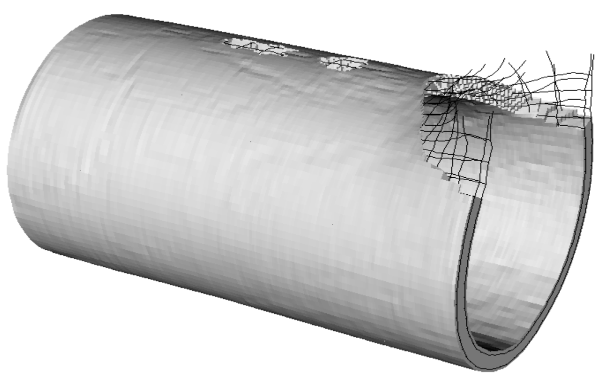

Figure 1. An example of a breached reinforced concrete tunnel (multiple breached zones)

AFTERBURN MODEL

Explosive afterburn is an additional energy release via combustion that can occur after an explosive detonates and is the result of detonation products mixing with oxygen at high temperature and pressure. Afterburn energy release can be substantial. For C-4, the heat of combustion is more than twice the detonation energy, so more energy can be theoretically released through afterburn than through detonation. The relevant timescales for the two types of explosive energy release are quite different, with detonation occurring on the scale of microseconds for ideal explosives and afterburn energy released on the time scale of milliseconds. The rate of energy release is dependent on temperature and pressure of the detonation products and the presence of oxygen with which to combust. A key challenge in modeling the effects of explosive afterburn is establishing the correct timescales and how much of the potential combustion energy is actually released. A bounding capability to assess the contribution of afterburn to structural loading, response and damage resulting from an explosive event has been developed based on barometric calorimeter tests and high-fidelity ALE3D simulations (Alves et al 2011). Barometric calorimeter tests of C-4 were conducted in nitrogen and air atmospheres. The air tests allowed for combustion of detonation products with ambient oxygen, while the nitrogen atmosphere suppresses afterburn. Comparing the tests isolates the energy release due to afterburn. Figure 2 shows representative calorimeter tests illustrating the effect of the afterburn on impulse measured at close range. For the first few milliseconds, the impulse is the same regardless of test atmosphere; however, the tests conducted in air quickly show increased impulse.

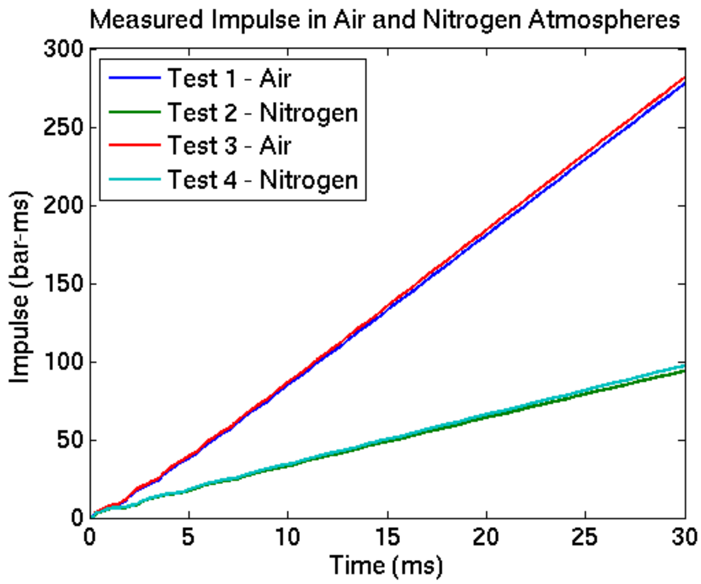

Figure 2. Specific impulse from barometric calorimeter tests in air and nitrogen atmospheres

The resulting model, termed the JWL-afterburn or JWLa, is an adaptation of the standard JWL equation of state to include a time-dependent term. The pressure given by the JWLa is

$$P_{JWLa} = P_{JWL} + \frac{E_{AB}}{v} Y_P(t)$$

where E_{AB} is the afterburn energy, v is the relative volume, and $Y_P(t)$ defines the time dependence of the energy release. The function $Y_P(t)$ takes the form $1\text{-}\exp(-t/\tau)$ where τ is the time constant for energy release. The model is set up to allow for a two-stage energy release, with different rates for each stage, to account for the effect of variable temperature and pressure following detonation on combustion rate.

AFTERBURN EFFECTS ON CLOSE-IN STRUCTURAL RESPONSE

The close-in structural response of a tunnel to an explosive including afterburn is investigated using the JWLa as implemented in ALE3D. The generic reinforced concrete tunnel used for the original breach analyses included in STUNTool (Glascoe et al 2012) is also used for this analysis, see Figure 1. The tunnel is 29.5ft long, has an inner radius of 90 inches, wall thickness of 30 inches and lies beneath 120 inches of cover soil. A spherical charge of C-4 explosive is used, with varying charge weight, standoff distance and rate of energy released via afterburn. Multiple simulations were performed to explore the effects of explosive afterburn and the sensitivity of the parameters of the afterburn model. For each case, a simulation without afterburn (using the standard JWL) and a simulation with afterburn (using JWLa) are performed.

Figure 3 shows the expected increase in pressure and impulse observed down-tunnel from the explosive source when afterburn is included in a simulation.

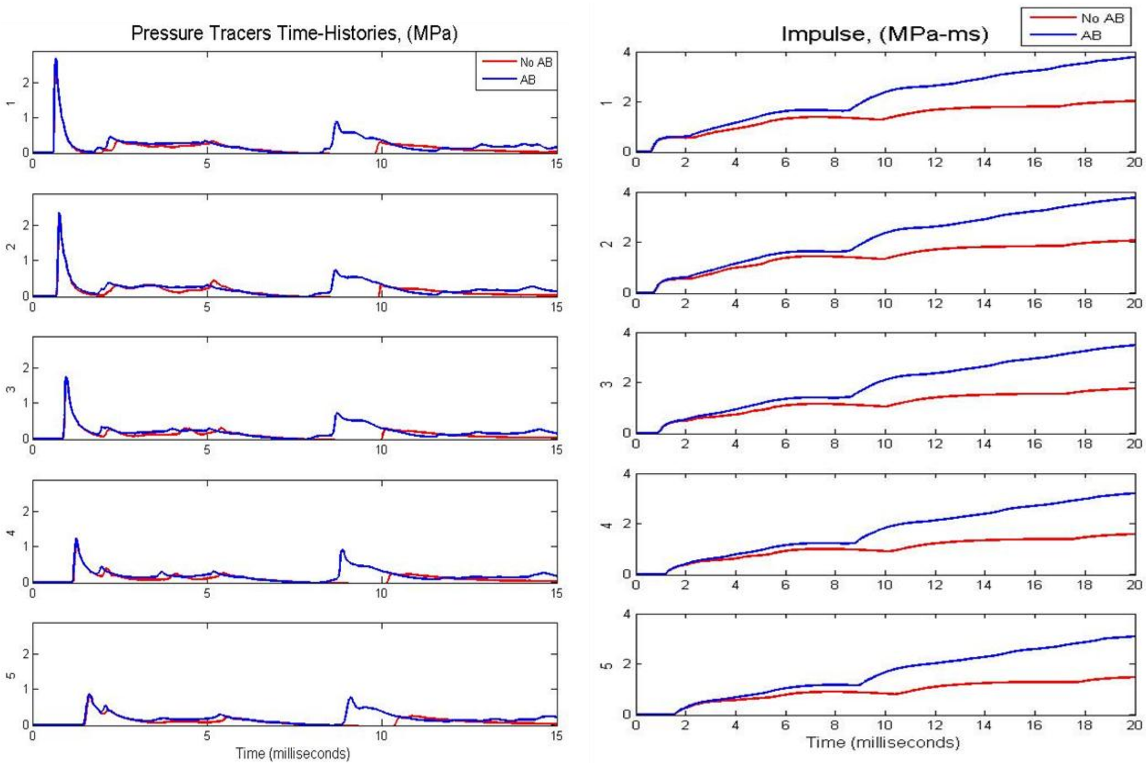

Figure 3. Pressure and impulse time histories for simulations with (red) and without afterburn (blue) for a series of locations down tunnel from the explosive source

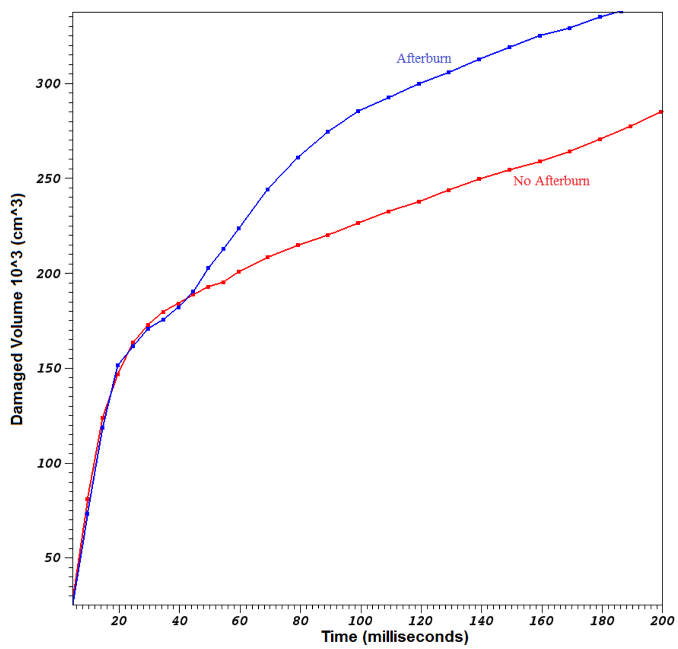

Figure 4. Total volume of damaged concrete over time for a small charge with small standoff

Figure 4 shows the total volume of damaged material in the tunnel wall that results for a small charge, small standoff case. The volume of damaged material for the afterburn simulation begins to surpass the volume of damaged material for the no-afterburn simulation at later times. A qualitative comparison showing which elements of the tunnel were damaged in otherwise equivalent simulations with and without afterburn is shown in Figure 5. This gives insight into where afterburn tends to generate damage on a tunnel wall.

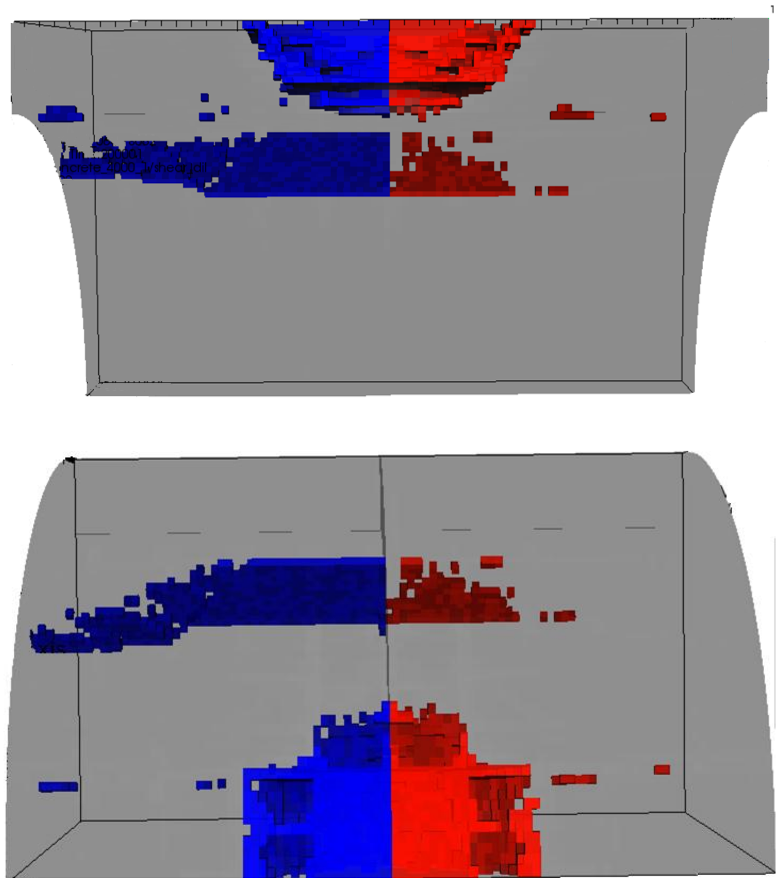

Figure 5. Side-by-side comparison of tunnel damage: damaged volume from the simulation with afterburn is shown in blue; damage from simulation without afterburn is shown in red

The results shown in Figure 3 to Figure 5 are representative of the results observed in this analysis. Figure 5 illustrates how adding afterburn to the simulation does not visibly increase the volume of damaged material in the area closest to the charge, where breach would be expected to occur (the possible breach area). However, the addition of afterburn visibly increases the volume of damaged material away from the possible breach area. The additional energy release contributes to the formation of new or larger cracks in portions of the tunnel wall relatively far from the initial explosion. The higher impulse from afterburn may also be causing increased rubble generation in already damaged areas. This behavior may increase the volume of damaged material without changing the breach assessment for the tunnel.

Figure 6 shows the damaged volume as a function of time for simulations with varying charge weight and constant standoff distance. The results shown in blue illustrate the damaged volume for the simulations that include afterburn while the red curves show the equivalent no afterburn simulations. As can be clearly seen, the effects of afterburn become more substantial as charge weight increases. Figure 7 shows the resulting damaged volume curves for cases with constant charge size but varying standoff. Decreasing standoff increases the effect of afterburn on the wall, as can be seen by the increasing gaps between afterburn and no afterburn curves. Some of these damage curves show that the simulations with afterburn had less damage at earlier times than the standard simulations, but the inclusion of afterburn eventually began to generate excess damage. This result for early time points is unexpected, though it may be due to increased pressure hardening of the concrete yield surface in the afterburn cases. Further studies into the early effects of the implementation of the afterburn model may be warranted.

In the simulations with varying charge weight or stand-off, the manner in which the additional afterburn damage occurs does not differ substantially from in Figure 5; the only visible increase in damage is outside the possible breach area and manifests as extra or larger cracks forming the in the tunnel wall.

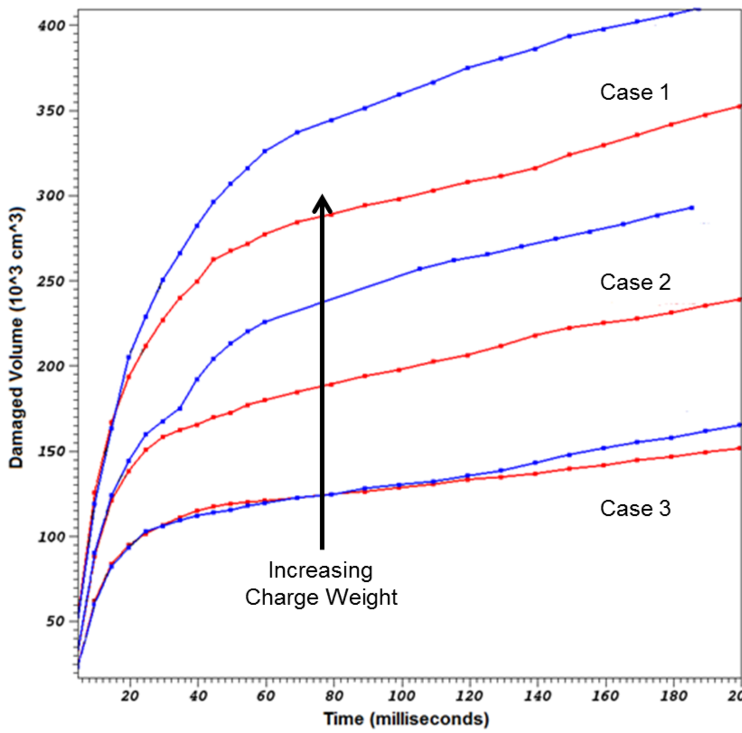

Figure 6. Damaged Volume for Varying Charge Weights (Blue=afterburn, Red=no afterburn)

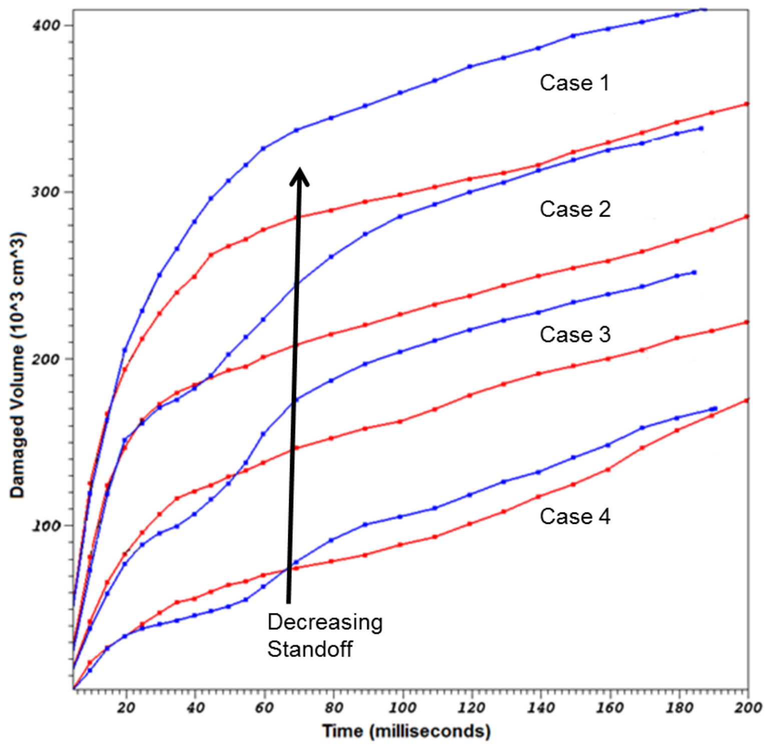

Figure 7. Damaged volume results for varying standoff distance (Blue=afterburn, Red=no afterburn)

VARYING JWL-A TIME CONSTANT

The amount of potential afterburn energy released can be varied through a pair of parameters in the JWLa model, however, as a bounding case in this study, the entire amount afterburn energy is released in a single stage. The parameter in the JWLa model which controls the timescale of the extra energy release is varied to explore the sensitivity of the tunnel damage model.

The time constant for the first stage of afterburn energy release is defined as: $\tau_1 = 8000 * m^{1/3}$, where *m* is the mass of the charge in kg. Since this relationship was developed for a different explosive than the one considered in this study (TNT and C-4, respectively), the sensitivity of this JWLa parameter was examined. The results for simulations with successively smaller coefficients for τ_1 are shown in Figure 8 and Figure 9. Figure 8 shows time histories of damaged volumes for a simulation without afterburn included in the model and for three simulations with afterburn, each with three different coefficients for τ_1: 8000 (the default value), 4000, and 2000. This reveals that using a smaller coefficient for the time constant leads to a larger damaged volume due to the more rapid release of afterburn energy. Figure 9 shows the qualitative results comparing each simulation with a different coefficient for τ_1 to a simulation without afterburn in the model. As the coefficient for τ_1 is decreased there is a visible increase in damaged material, but, as before, the additional damaged material is not near the possible breach area.

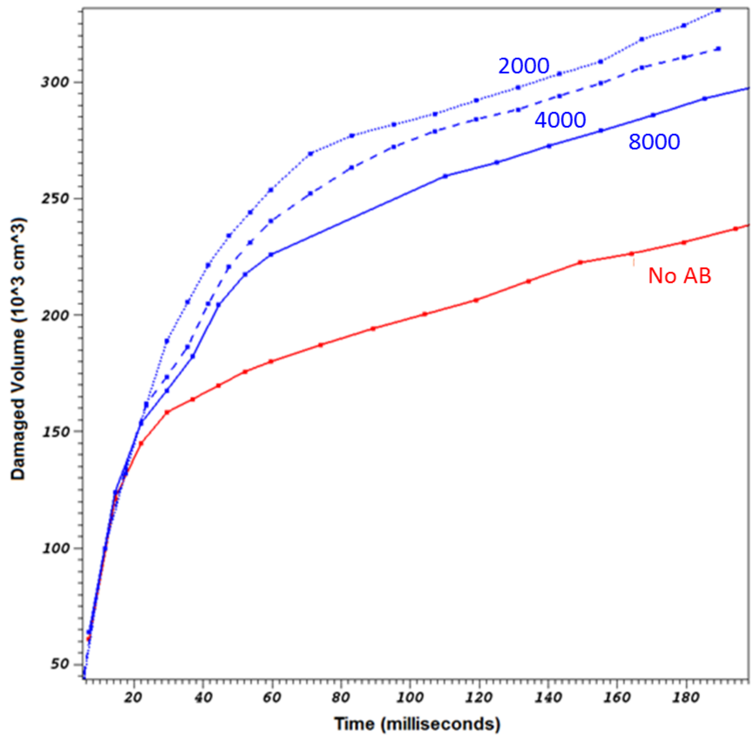

Figure 8. Volume of damaged tunnel material for simulations with different first stage time coefficients

CONCLUSIONS

Including afterburn in the ALE3D tunnel simulations results in higher pressures and impulses down-tunnel and causes more damage to the tunnel wall at later times. This was an expected result, as including afterburn in the model provides an additional release of energy. However, while the results show that the inclusion of afterburn leads to more total damage, there is no obvious increase of damage around the possible breach area for any of the cases investigated. In all cases considered, the additional damage due to afterburn manifested by enlarging existing cracks or by forming new cracks away from the potential breach area. Changing the time over which the additional energy release occurs, by reducing the coefficient in the τ_1 expression, results in larger overall volume of damaged material, but once again did not result in a larger predicted breach area.

The purpose of this study was to analyze the effects of afterburn and to see if the inclusion of afterburn in simulations would alter the breach assessment for a tunnel, and therefore require an adjustment of the exitsing breach curves in STUNTool. As the full potential of afterburn energy was released in these simulations as a bounding “worst case” and still no additional damage was observed in the potential breach area, the existing STUNTool breach curves should not require modification.

FUTURE WORK

Utilizing the currently available model to account for the release of afterburn energy does not indicate the need to change the breach characterization method present in the tool. However, the additional energy release does change the overpressure and impulse down tunnel from the explosive source and will affect estimates of personnel injuries and damage to secondary structures within the tunnel. Efforts are currently underway to adopt the modified JWLa for use in the 1D STUN code in order to account for afterburn energy release.

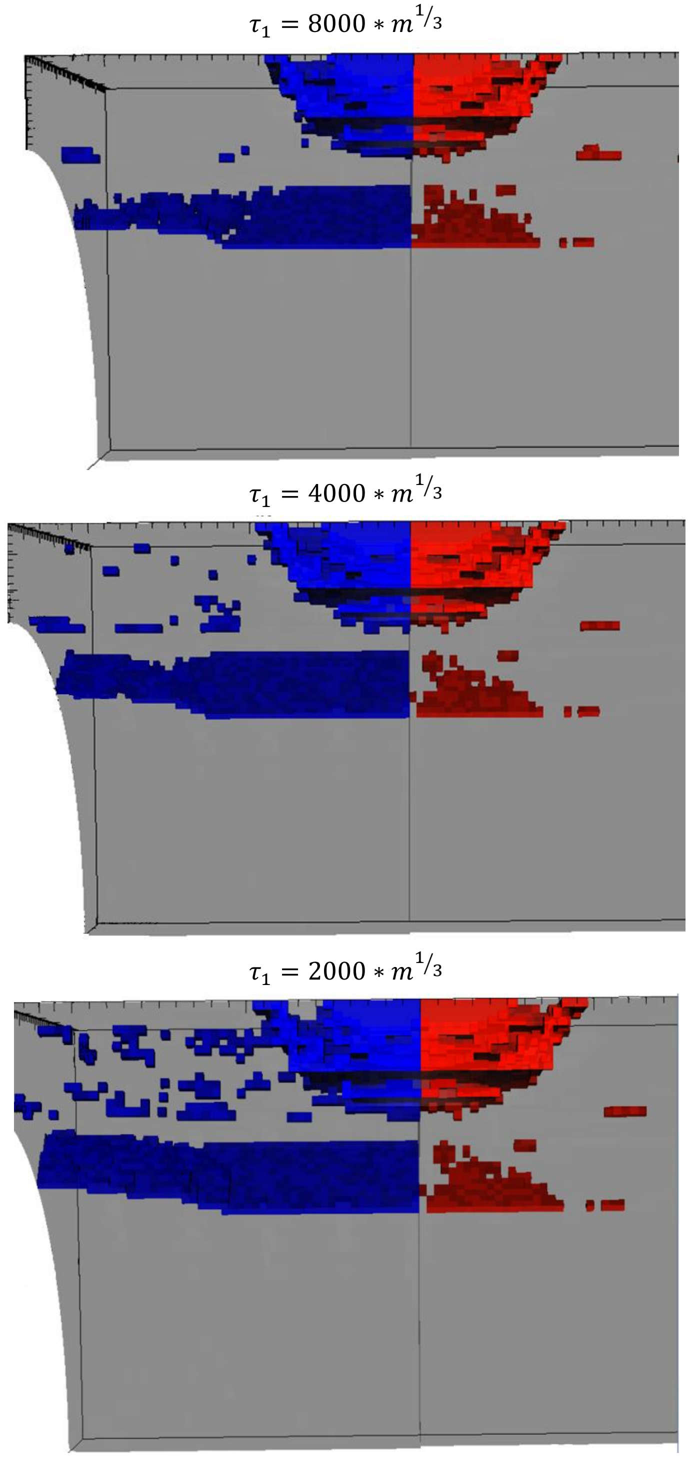

Figure 9. Tunnel damages for various τ_1 coefficients (from top: 8000, 4000, 2000). Results from simulations with afterburn are shown in blue, results from simulation without afterburn are shown in red.

ACKNOWLEDGMENTS

This work is performed under the auspices of the U.S. Department of Energy by Lawrence Livermore National Laboratory under Contract DE-AC52-07NA27344. We would like to thank the Department of Homeland Security's Science and Technology Directorate (DHS S&T) and the Transportation Security Administration for their sponsorship and assistance in these efforts. We particularly acknowledge the assistance and leadership of Dr. John Fortune (DHS S&T) and Mr. Christopher McKay (TSA).

REFERENCES

Alves, S., Kuhl, A., Najjar, F., Tringe, J., McMichael, L., Glascoe, L. (2011) "Building an Efficient Model for Afterburn Energy Release." 82nd Shock & Vibration Symposium, October 31-November 3, Baltimore, Maryland.

Glascoe, L., Neuscamman, S., Lennox, K., Elmer, W., Glenn, L., and McMichael, L. (2012) "A Fast-running tool to characterize shock damage on structures." Proceedings for ASCE Structures Congress, Chicago, IL March 29-31

Glascoe, L. Elmer, W. Glenn, L., Kupresanin, A., McMichael, L., and Minkoff, S. (2011), Proceedings for DHS University Summit, Washington, D.C., February 7.

Glascoe, L., Noble, C., Reynolds, J.G., Kuhl, A., and Morris, J. (2009). "Securing Transportation Systems from High Explosive Threats." Proceedings of the 2009 IEEE International Conference on Technologies for Homeland Security, May 11-12, Waltham, MA, LLNL-PROC-411500.

Glenn, L. A. (2001). "Simulating MARVEL with the STUN Code." LLNL UCRL-ID-143993 (June 6, 2001).

Lennox, K. P. and Glascoe L. (2011). "Constrained Classification for Infrastructure Threat Assessment.", In: Proceedings for the IEEE International Conference on Technologies for Homeland Security, 15-17 November, Waltham, MA.

McGlaun, J.M., M.G. Thompson, and M.G. Elrick. (1990). "CTH: a three-dimensional shockwave physics code." *Int. J. Impact Engng,* Vol. 10: 351-360.

Neuscamman, S., Glenn, L. and Glascoe, L. (2011). "A Fast-Running, Physics-Based Tool for Explosives in Tunnels: Model Validation" Presented at 82nd Shock & Vibration Symposium, October 31-November 3, Baltimore, Maryland. LLNL-PRES-509019

Nichols, A. L. and the ALE3D team (2009). Users Manual for ALE3D, An Arbitrary Lagrange/Eulerian 2D and 3D Code System, Volume 2, Material and Chemical Models, Lawrence Livermore National Laboratory, UCRL-SM-404490.